Hamburger Beiträge
zur Angewandten Mathematik

A kinetic scheme for the Savage-Hutter equations

Christine Kaland and Jens Struckmeier

Nr. 2007-15
October 2007

A kinetic scheme for the Savage-Hutter equations

Christine Kaland [*], Jens Struckmeier [†]

Abstract: The Savage-Hutter equations describe the motion of granular material under the influence of friction. Based on the kinetic formulation of the Savage-Hutter equations we present a kinetic scheme in one dimension, which describes the deformation of the mass profile and allows it to start and to stop. Moreover the method is able to preserve the steady states of granular masses at rest. The method is testet on several numerical examples.

Keywords: Kinetic schemes, kinetic formulation, Savage-Hutter equations, finite volume schemes.

1 Introduction

Dense snow avalanches and landslides regularly entail enormous damage. Therefore it would be extremely helpful if one could predict the dynamic behaviour of such granular masses, particularly to predict the place, where the mass comes to rest.
Furthermore, industrial problems dealing with the dynamic behaviour of granular material like the modeling of grain in silos are of great interest.
In [10] Savage and Hutter deduce a model based on the incompressible Euler equations to describe the dynamic of such granular masses moving on a bottom topography, which is constant in time and spatially only slowly varying. Under the additional assumption that the internal friction angle equals the dynamic friction angle the Savage-Hutter equations read

$$\begin{aligned} \partial_t h + \partial_x (hu) &= 0 \ , \\ \partial_t (hu) + \partial_x (hu^2 + \beta \frac{h^2}{2}) &= g\, h \ , \end{aligned} \tag{1}$$

where

$$\beta = \varepsilon\, k\, \cos\zeta$$

and

$$g = g(u) = \sin\zeta - \mathrm{sgn}\,(\mathrm{u})\, \cos\zeta\, \tan\delta \quad \text{for u} \neq 0$$

in the unknowns $h, hu : \mathbb{R} \times (0, \infty) \longrightarrow \mathbb{R}$. Thereby h and u denote the height of the granular material and its average velocity, respectively. Moreover ζ is referred to as the inclination

[*]Universität Hamburg, Department Mathematik, Schwerpunkt Differentialgleichungen und Dynamische Systeme, Bundesstraße 55, 20146 Hamburg, Germany, christine.kaland@math.uni-hamburg.de

[†]Universität Hamburg, Department Mathematik, Schwerpunkt Differentialgleichungen und Dynamische Systeme, Bundesstraße 55, 20146 Hamburg, Germany, struckmeier@math.uni-hamburg.de

angle of the basement topography against the horizontal, δ denotes the dynamic friction angle, ε the ratio of characteristic height to characteristic lenght of the mass under consideration and k is an earth pressure coefficient. The system is hyperbolic as long as the height stays nonnegative. In [11] this model is extended to smoothly varying bottom topographies which results in an additional x-dependence in the flux function. The effect of friction is modelled in both equations by a simple Coulomb model. Other friction models that are not subject to this paper are discussed in [5]. For simplification the Savage-Hutter equations are in the following abbreviated by SH equations.

The source term $g\,h$ on the right hand side of the second equation of (1) causes nonconstant steady states, that actually do make sense physically. But in contrary to other models for fluid dynamic processes like the shallow water equations, there are infinitly many of such steady states, which are described by

$$\partial_t h = 0 \ , \quad u = 0 \ . \tag{2}$$

If we insert (2) into the SH equations (1), we get the following relation between the spatial derivative of h and the source term

$$\beta\, \partial_x h = g \ .$$

Since we are interested in granular masses at rest, we have to consider static friction instead, which is bounded by the dynamic friction because of the Coulomb model. Therefore the source term and therewith the steady states are not uniquely defined for $u = 0$, but we can give a simple criterion on $\partial_x h$ to decide whether the mass is in equilibrium or not. Height profiles h, which satisfy that condition are named admissible profiles in the following. An exact definition of admissible profiles is given in section 3.

The aim of this paper is to present a numerical scheme based on a kinetic Ansatz for the SH equations, that preserves such steady states and is able to describe the beginning of sliding and the stopping of more general solutions. Moreover we can apply a stability result from [8], that ensures the nonegativity of the height under few conditions.

In the next section we present the (semi-)kinetic formulation of both the simplified SH equations with $\beta = const$ and the generalized SH equations for smoothly varying chutes. For the constuction of the kinetic formulations we use an Ansatz of Perthame and Simeoni presented in [8]. The conservative and consistent scheme with the desired properties is constructed in the third section. In the fourth section the method is tested on several examples. A conclusion of the results and an outlook to possible extensions are given at the end of the paper.

2 The kinetic formulation

In this section we present a kinetic formulation for both the simlified SH equations with constant inclination angle and the general equations describing the motion of granular material down a smooth chute as explained in the introduction.

2.1 The kinetic formulation for a constant inclination angle

Let us first consider a constant inclination angle $\zeta = const$ and therefore $\beta = const$. Similar to the kinetic formulation of the Euler equations or the shallow water equations in [2], [7] and [8], we are looking for a density of particles $M(x, \xi, t) = M(h, \xi - u)$ satisfying

$$\begin{pmatrix} h \\ hu \\ hu^2 + \frac{1}{2}\beta h^2 \end{pmatrix} = \int_{\mathbb{R}} \begin{pmatrix} 1 \\ \xi \\ \xi^2 \end{pmatrix} M(h, \xi - u)\, d\xi \ . \tag{3}$$

In the following we proceed as Perthame and Simeoni in [8] for the shallow water equations and define M by making the Ansatz

$$M(h, \xi - u) = \sqrt{h}\ \chi\Big(\frac{\xi - u}{\sqrt{h}}\Big) \tag{4}$$

with a nonnegative function $\chi : \mathbb{R} \to \mathbb{R}$ satisfying

$$\begin{aligned} \chi(\omega) &= \chi(-\omega) \ , \\ \int_{\mathbb{R}} \chi(\omega)\, d\omega &= 1 \ , \\ \int_{\mathbb{R}} \omega^2\, \chi(\omega)\, d\omega &= \frac{\beta}{2} \ . \end{aligned} \tag{5}$$

It is easy to see, that every function M of the form (4) satisfies (3): because of the properties (5) we obtain for the moments of M

$$\begin{aligned} \int_{\mathbb{R}} M(h, \xi - u)\, d\xi &= \int_{\mathbb{R}} \sqrt{h}\ \chi\Big(\frac{\xi - u}{\sqrt{h}}\Big)\, d\xi \\ &= \int_{\mathbb{R}} \sqrt{h}\ \chi(\omega)\sqrt{h}\, d\omega \\ &= h \int_{\mathbb{R}} \chi(\omega)\, d\omega \\ &= h \ , \\ \int_{\mathbb{R}} \xi\, M(h, \xi - u)\, d\xi &= \int_{\mathbb{R}} \xi\, \sqrt{h}\ \chi\Big(\frac{\xi - u}{\sqrt{h}}\Big)\, d\xi \\ &= \int_{\mathbb{R}} (\sqrt{h}\omega + u)\ \sqrt{h}\ \chi(\omega)\sqrt{h}\, d\omega \\ &= h^{3/2} \int_{\mathbb{R}} \omega\, \chi(\omega)\, d\omega + hu \int_{\mathbb{R}} \chi(\omega)\, d\omega \\ &= hu \int_{\mathbb{R}} \chi(\omega)\, d\omega \\ &= hu \ , \end{aligned}$$

$$\begin{aligned}
\int_{\mathbb{R}} \xi^2\, M(h,\xi-u)\, d\xi &= \int_{\mathbb{R}} \xi^2 \sqrt{h}\, \chi\Big(\frac{\xi-u}{\sqrt{h}}\Big)\, d\xi \\
&= \int_{\mathbb{R}} (\sqrt{h}\,\omega+u)^2\ \sqrt{h}\ \chi(\omega)\sqrt{h}\, d\omega \\
&= h^2 \int_{\mathbb{R}} \omega^2\, \chi(\omega)\, d\omega + 2\ h^{3/2} u \int_{\mathbb{R}} \omega\, \chi(\omega)\, d\omega + hu^2 \int_{\mathbb{R}} \chi(\omega)\, d\omega \\
&= hu^2 + \frac{1}{2}\beta h^2\ .
\end{aligned}$$

These relations lead to the following theorem, the same theorem as Perthame and Simeoni formulate in [8] for the shallow water equations.

Theorem 1 *The pair (h, hu) is a solution of the equation (1), if and only if $M(h,\xi-u)$ of the form (4) solves the kinetic equation*

$$\partial_t M(h,\xi-u) + \xi\, \partial_x M(h,\xi-u) + g(u)\, \partial_\xi M(h,\xi-u) =: Q(t,x,\xi) \tag{6}$$

with $Q(t,x,\xi)$ satisfying

$$\int_{\mathbb{R}} Q\, d\xi = 0 \quad \textit{und} \quad \int_{\mathbb{R}} \xi\, Q\, d\xi = 0 \tag{7}$$

Proof. If (h, hu) is a solution of (1) and M of the form (4), equation (6) is satisfied by definition. Because of the properties (3) it is easy to see that the collision operator Q meets the conditions (7).
Let now be M of the form (4) and (h, hu) such that $M(h,\xi-u)$ solves the equation (6) with Q satisfying (7). We then integrate (6) with respect to ξ and use again the properties (3) to see that (h, hu) solves equation (1). □

Remark 1 *Note that there are still macroscopic values in the kinetic equation (6). Therefore the Vlasov type equation (6) is often called a kinetic representation or semi-kinetic formulation instead of kinetic formulation (see [7]).*

Remark 2 *The only nonlinearity of equation (6) is caused by the collision operator Q. Therefore (6) is a lot easier to handle than the original system.*

Now we have to choose the function χ. In contrast to the shallow water equations, where friction is neglected and the only physical staedy states are those of a "lake at rest", the SH equations admit infinitly many steady states of granular masses at rest. It is clear that the height profile of such a granular mass is not uniquely defined, moreover the gradient of the profile has to be somehow bounded to avoid the moving of the material. But if one inserts the criterion $\partial_t h = 0$ and $u = 0$ for a mass at rest into the SH equations, one finds the following relation between the height h and the function g

$$\beta\ \partial_x h = g\ . \tag{8}$$

Note that g is not yet defined for $u = 0$, as described in the introduction. Nevertheless, for $u = 0$ the values of g do not exceed certain bounds because g is defined as the sum of a gravitational force term

$$g_1 := \sin\zeta$$

and a second term, which expresses the Coulomb friction

$$g_2 := -\frac{u}{|u|}\cos\zeta\,\tan\delta \quad \text{for } u \neq 0\ .$$

In a simple Coulomb friction model the static friction does not exceed the dynamic friction and therefore

$$-\cos\zeta\,\tan\delta \leq g_2 \leq \cos\zeta\,\tan\delta \quad \text{for } u = 0\ .$$

Moreover we demand the collision operator Q to vanish in equilibrium. This condition does make sense in analogy to classical gas dynamics since up to here the only constraint on Q is the vanishing of the first two moments.
Therefore for steady states of the form $\partial_t h = 0$ and $u = 0$ equation (6) becomes

$$\xi\,\partial_x M(h,\xi) + g\,\partial_\xi M(h,\xi) = 0\ . \tag{9}$$

As described in [8] one can convert this equation into an ordinary differential equation for χ using (8) and the substitution $\omega = \xi/\sqrt{h}$:

$$\begin{aligned} & \tfrac{\partial_x h}{2}\Big[\tfrac{\xi}{\sqrt{h}}\chi\Big(\tfrac{\xi}{\sqrt{h}}\Big) - \tfrac{\xi^2}{h}\chi'\Big(\tfrac{\xi}{\sqrt{h}}\Big) + g\tfrac{2}{\partial_x h}\chi'\Big(\tfrac{\xi}{\sqrt{h}}\Big)\Big] &= 0 \\ \Leftrightarrow\quad & \tfrac{\partial_x h}{2}\Big[\omega\chi(\omega) - \omega^2\chi'(\omega) + 2\beta\chi'(\omega)\Big] &= 0 \\ \Leftrightarrow\quad & \Big[\omega\chi(\omega) + (2\beta - \omega^2)\chi'(\omega)\Big] &= 0 \end{aligned} \tag{10}$$

Under the conditions (5) equation (10) admits the unique solution

$$\chi(\omega) = C\,\sqrt{\left(2\beta - \omega^2\right)_+} \quad \text{where} \quad C = \frac{1}{\pi\beta}\ . \tag{11}$$

Finally the microscopic equilibrium density for a constant inclination angle is specified by

$$\begin{aligned} M(h,\xi-u) &= \sqrt{h}\,\chi\Big(\frac{\xi-u}{\sqrt{h}}\Big) \\ &= \frac{\sqrt{2h}}{\pi\sqrt{\beta}}\sqrt{\Big(1 - \frac{(\xi-u)^2}{2\beta h}\Big)_+}\ . \end{aligned} \tag{12}$$

Of course, this is the same result as in [8] for the shallow water equations.
To preserve the steady states numerically, the discretisation of the kinetic equation and particularly that of the source term are extremely important. In [8] the authors construct a scheme with reflections following the concept of upwinding the sources at interfaces as described in [3] and [9]. In this paper we do not follow this concept since friction is a volumic force rather than an interface force and the interpretation as a surface effect is not evident. But away from physical meaning there are ideas to treat friction as a bottom topography (see [4]). The discretization for equation (6) is elaborated in section 3, but first we want to give the kinetic formulation for the more general case of smoothly varying chutes.

2.2 The kinetic formulation for smooth chutes

In this section we consider the general SH equations for smoothly varying inclination angles $\zeta(x)$

$$
\begin{aligned}
\partial_t h + \partial_x(hu) &= 0 \ , \\
\partial_t(hu) + \partial_x(hu^2 + \beta\frac{h^2}{2}) &= gh \ ,
\end{aligned}
\tag{13}
$$

where

$$\beta = \beta(x) = \varepsilon\, k\, \cos\zeta(x)$$

and

$$g = g(u,x) = \sin\zeta(x) - \operatorname{sgn}(u)\, \tan\delta\, (\cos\zeta(x) + \eta\kappa(x)u^2) \quad \text{for } u \neq 0 \ .$$

Here the quantity κ denotes the curvature of the chute and $\eta = \frac{L}{R}$ is known as the characteristic curvature where R denotes the radius of curvature of the chute. For simplicity we made again the assumption that the internal friction angle equals the dynamic friction angle. To get a kinetic formulation with a preferably simple function χ, we first transform the system (13) such that the only dependence of the spatial variable x occurs on the right hand side (see [1]).
Presuming that β is differentiable and $\gamma := \beta^{'}/\beta$ exists the system reads in the new variables $\rho := \beta h$ and $m := \beta h u$

$$\partial_t v + \partial_x F(v) = G(v,x) \ , \tag{14}$$

where

$$v = \begin{pmatrix} \rho \\ m \end{pmatrix} ,$$

$$F(v) = \begin{pmatrix} m \\ m^2/\rho + \rho^2/2 \end{pmatrix}$$

and

$$G(v,x) = \begin{pmatrix} \gamma\, m \\ \gamma\,(m^2/\rho + \rho^2/2) + \rho\, g \end{pmatrix} .$$

In analogy to the previous section we are looking for a density $M(\rho, \xi - m/\rho) = \sqrt{\rho}\,\chi(\frac{\xi - m/\rho}{\sqrt{\rho}})$, that satisfies

$$\int_{\mathbb{R}} \begin{pmatrix} 1 \\ \xi \\ \xi^2 \end{pmatrix} M(\rho, \xi - m/\rho)\, d\xi = \begin{pmatrix} \rho \\ m \\ m^2/\rho + \rho^2/2 \end{pmatrix} . \tag{15}$$

Choosing χ as a nonnegative function, that meets the conditions

$$\begin{aligned} \chi(\omega) &= \chi(-\omega) \ , \\ \int_{\mathbb{R}} \chi(\omega)\, d\omega &= 1 \ , \\ \int_{\mathbb{R}} \omega^2\, \chi(\omega)\, d\omega &= \frac{1}{2} \ , \end{aligned} \tag{16}$$

the conditions (15) are always satisfied. For the new variables ρ and m we get the following theorem.

Theorem 2 *The pair (ρ, m) is a solution of the equation (14), if and only if $M(\rho, \xi - m/\rho) = \sqrt{\rho}\, \chi(\frac{\xi - m/\rho}{\sqrt{\rho}})$, where χ fulfills (16), solves the kinetic equation*

$$\partial_t M + \xi\, \partial_x M + \left[\frac{\gamma}{2}\left(\xi^2 - \left(\frac{m^2}{\rho^2} + \frac{\rho}{2}\right)\right) + g\right] \partial_\xi M = Q \tag{17}$$

with $Q(t, x, \xi)$ satisfying

$$\int_{\mathbb{R}} Q\, d\xi = 0 \quad \textit{and} \quad \int_{\mathbb{R}} \xi\, Q\, d\xi = 0 \ .$$

Proof. The equations (6) and (17) differ only in the coefficient

$$F(x, \xi, t) = \frac{\gamma}{2}\left(\xi^2 - \left(\frac{m^2}{\rho^2} + \frac{\rho}{2}\right)\right) + g$$

in front of $\partial_\xi M$. This force term has to satisfy

$$\int_{\mathbb{R}} \begin{pmatrix} 1 \\ \xi \end{pmatrix} F(x, \xi, t)\ \partial_\xi M(\rho, \xi - m/\rho)\, d\xi = - \begin{pmatrix} \gamma\, m \\ \gamma\, (m^2/\rho + \rho^2/2) + \rho\, g \end{pmatrix} \ .$$

Because of the compact support of M we obtain

$$\begin{aligned} \int_{\mathbb{R}} F\ \partial_\xi M\, d\xi &= \frac{\gamma}{2} \int_{\mathbb{R}} \xi^2\, \partial_\xi M\, d\xi + \left(g - \frac{\gamma}{2}\left(\frac{m^2}{\rho^2} + \frac{\rho}{2}\right)\right) \int_{\mathbb{R}} \partial_\xi M\, d\xi \\ &= -\frac{\gamma}{2} \int_{\mathbb{R}} 2\, \xi\, M\, d\xi \\ &= -\gamma\, m \end{aligned}$$

and

$$\begin{aligned} \int_{\mathbb{R}} \xi\, F\, \partial_\xi M\, d\xi &= \frac{\gamma}{2} \int_{\mathbb{R}} \xi^3\, \partial_\xi M\, d\xi + \left[g - \frac{\gamma}{2}\left(\frac{m^2}{\rho^2} + \frac{\rho}{2}\right)\right] \int_{\mathbb{R}} \xi\, \partial_\xi M\, d\xi \\ &= -\frac{\gamma}{2} \int_{\mathbb{R}} 3\, \xi^2\, M\, d\xi + \left[\frac{\gamma}{2}\left(\frac{m^2}{\rho^2} + \frac{\rho}{2}\right) - g\right] \int_{\mathbb{R}} M\, d\xi \\ &= -\frac{3}{2}\gamma \left(\frac{m^2}{\rho} + \frac{\rho^2}{2}\right) + \frac{\gamma}{2}\left(\frac{m^2}{\rho^2} + \frac{\rho}{2}\right) \rho - \rho g \\ &= -\gamma \left(\frac{m^2}{\rho} + \frac{\rho^2}{2}\right) - \rho\, g \ . \end{aligned}$$

□

Unfortunately for equation (17) it is not as easy as before to specify an equilibrium density M. In equation (6) we were able to eliminate the disturbing macroscopic values to fix the function χ. The method presented in the next section is based only on the results for a constant inclination angle. Therefore in the following the density M is assumed to be of the special form (12). Some ideas to handle smoothly varying bottom topographies are given in section 5.

3 A quasi-balanced scheme in 1D

In this section we present a finite volume scheme in one dimension for the SH equations (1) based on the kinetic formulation, i.e. a numerical method that preserves the steady states of a granular mass at rest. Furthermore it can be shown easily that the scheme preserves the nonnegativity of the materials' height at least in regions of large deformations.

For the construction of the scheme we proceed as follows: at first we present a microscopic finite volume scheme in one dimension for the kinetic formulation of the SH equations. Integration of the method leads to a consistent macroscopic scheme, which is conservative and in some sense stable in the first component (scheme 1). This method is not able to preserve the steady states, but with little modifications of the microscopic flux function and the discretization of the source term we obtain a scheme with the desired property. Successively this method will be modified so that the resulting scheme is able to describe the stopping of the mass, too (scheme 2). Unfortunately the corrected method generates oscillations for highly inadmissible initial profiles like Riemann data. Since the second scheme was only constructed to describe the starting and stopping of the granular mass, we combine the two schemes and use the second one for the starting and stopping process and the first one otherwise.

3.1 A first microscopic scheme

First we want to discretize equation (6). Therefore we consider an equidistant mesh of $\mathbb{R} \times (0, \infty)$ with points $(x_i, t_n) = (i\Delta x, n\Delta t)$, $i \in \mathbb{Z}$, $n \in \mathbb{N}$. The cell C_i is defined as $C_i = [x_{i-1/2}, x_{i+1/2}]$, where the interfaces are $x_{i+1/2} = (x_i + x_{i+1})/2$. The length of such a control volume is denoted by Δx, the time step by Δt. In each point (x_i, t_n) we denote by the approximations $(h_i^n, q_i^n = (hu)_i^n)$ the cell averages over the cell C_i.
Moreover we define

$$u_i^n = \frac{q_i^n}{h_i^n}$$

and

$$U_i^n = \begin{pmatrix} h_i^n \\ q_i^n \end{pmatrix} .$$

With these quantities the discrete density of particles $M_i^n(\xi)$ is given by

$$M_i^n(\xi) = M(h_i^n, \xi - u_i^n)$$

In order to discretize equation (6) we firstly neglect the collision operator Q and get

$$f_i^{n+1}(\xi) - M_i^n(\xi) + \lambda\xi\left(M_{i+1/2}^n(\xi) - M_{i-1/2}^n(\xi)\right) + \Delta t\, g_i^n\,(M_\xi)_i^n(\xi) = 0 \tag{18}$$

where $\lambda = \Delta t/\Delta x$ and the microscopic fluxes $M_{i+1/2}^n$ are defined by the Upwind formula

$$M_{i+1/2}^n = \begin{cases} M_i^n(\xi) & \text{für } \xi \geq 0, \\ M_{i+1}^n(\xi) & \text{für } \xi < 0. \end{cases} \tag{19}$$

Because neglecting the collision operator the density $f_i^{n+1}(\xi)$ is no longer an equilibrium density, i.e. it satisfies no longer the conditions (3). Therefore the resulting density is denoted by $f_i^{n+1}(\xi)$ instead of M_i^{n+1}, but can be projected back to the class of equilibrium densities via

$$U_i^{n+1} := \int_{\mathbb{R}} \begin{pmatrix} 1 \\ \xi \end{pmatrix} f_i^{n+1}(\xi)\, d\xi \tag{20}$$

This procedure is a common practice in constructing kinetic schemes (see [7], [8]).

The microscopic density $M_i^{n+1}(\xi)$ is obtained from the data at time level t_n as follows:

1. receive $f_i^{n+1}(\xi)$ from equation (18),
2. compute the macroscopic quantity $U_i^{n+1} = \left(h_i^{n+1}, q_i^{n+1}\right)^T$ via (20),
3. the density $M_i^{n+1}(\xi) = M(h_i^{n+1}, \xi - u_i^{n+1})$ is an equilibrium density again, i.e. it satisfies (3).

To discretize the source term we simply choose $g_i^n = g(u_i^n)$ for $u_i^n \neq 0$. For $u = 0$ the function $g(u)$ is not defined, but is in relation to the spatial derivative via $\beta\,\partial_x h = g$. Therefore, for $u = 0$, the source term should be discretized as

$$g_i^n = \beta\left(\frac{h_{i+1}^n - h_{i-1}^n}{2\Delta x}\right) . \tag{21}$$

Additionally we know that static friction is bounded by dynamic friction. These facts motivate the following definition.

Definition 1 (admissible profile) *A mass profile h is said to be admissible, if its spatial derivative $\partial_x h$ satisfies*

$$\min\left[\sin\zeta + R,\, \max\left(\beta\,\partial_x h,\, \sin\zeta - R\right)\right] = \beta\,\partial_x h$$

where $\pm R$ denotes the force term resulting from friction and

$$R = \cos\zeta\,\tan\delta\ .$$

The discretized version of that definition can be chosen as:

$$\min\left[\sin\zeta + R,\, \max\Big(\beta\left((h^n_{i+1} - h^n_{i-1})/2\Delta x\right),\, \sin\zeta - R\Big)\right] = \beta\left((h^n_{i+1} - h^n_{i-1})/2\Delta x\right)\ . \quad (22)$$

If relation (22) does not hold, the mass profile is not considered to be in equilibrium. In this case g_i^n should be set to one of the bounds. Overall we obtain for g_i^n

$$g_i^n = \begin{cases} \tilde{g}_i^n & \text{if} \quad u_i^n = 0 \\ g(u_i^n) & \text{otherwise} \end{cases}$$

where

$$\tilde{g}_i^n = \min\left[\sin\zeta + R,\, \max\Big(\beta\left((h^n_{i+1} - h^n_{i-1})/2\Delta x\right),\, \sin\zeta - R\Big)\right]\ .$$

Instead of (18) we will use the microscopic scheme

$$f_i^{n+1}(\xi + \Delta t g_i^n) - M_i^n(\xi) + \lambda\xi\left(M^n_{i+1/2}(\xi) - M^n_{i-1/2}(\xi)\right) = 0 \quad (23)$$

in further considerations.

3.2 A macroscopic scheme

We now get a macroscopic scheme by computing the first two moments of (23). Because of

$$\int_{\mathbb{R}} \xi\, f_i^{n+1}(\xi + \Delta t\, g_i^n)\, d\xi = \int_{\mathbb{R}} (\xi - \Delta t\, g_i^n)\, f_i^{n+1}(\xi)\, d\xi = (hu)_i^{n+1} - \Delta t\, g_i^n\, h_i^{n+1}$$

we obtain

$$\begin{aligned} U_i^{n+1} &= U_i^n - \lambda\left(F^n_{i+1/2} - F^n_{i-1/2}\right) + \Delta t\, S_i^n \\ \text{mit} \quad S_i^n &= \begin{pmatrix} 0 \\ g_i^n\, h_i^{n+1} \end{pmatrix}\ . \end{aligned} \quad (24)$$

Thereby the macroscopic fluxes are given by

$$\begin{aligned} F^n_{i+1/2} &= F(U_i^n, U_{i+1}^n) \\ &= \int_{\xi\geq 0} \xi \begin{pmatrix} 1 \\ \xi \end{pmatrix} M_i^n(\xi)\, d\xi + \int_{\xi<0} \xi \begin{pmatrix} 1 \\ \xi \end{pmatrix} M^n_{i+1}(\xi)\, d\xi\ . \end{aligned}$$

After some easy calculation we obtain for the first component of $F^n_{i+1/2}$

$$
\begin{aligned}
(F^n_{i+1/2})^1 &= \int_{\xi\geq 0} \xi\, M^n_i(\xi)\, d\xi + \int_{\xi<0} \xi\, M^n_{i+1}(\xi)\, d\xi \\
&= \underbrace{\int_{\xi\geq 0} \xi\, M(h^n_i, \xi - u^n_i)\, d\xi}_{I_1} + \underbrace{\int_{\xi<0} \xi\, M(h^n_{i+1}, \xi - u^n_{i+1})\, d\xi}_{I_2}
\end{aligned}
$$

where

$$
\begin{aligned}
I_1 &= \int_{\xi\geq 0} \xi \sqrt{h^n_i}\, \chi\Big(\frac{\xi - u^n_i}{\sqrt{h^n_i}}\Big)\, d\xi \\
&= \sqrt{h^n_i}\, \frac{\sqrt{2}}{\pi\sqrt{\beta}} \int_{\xi\geq 0} \xi \left(1 - \left(\frac{\xi - u^n_i}{\sqrt{2\beta h^n_i}}\right)^2\right)^{1/2}_{+} d\xi \\
&= \begin{cases}
(hu)^n_i & \text{if} \quad a_1 \leq -1 \\[2ex]
\frac{2}{3\pi}\sqrt{2\beta}\,(h^n_i)^{3/2}\ \cos^3(\arcsin(a_1)) & \\
+\frac{2}{\pi}\,(hu)^n_i \left(\frac{\pi}{4} - \frac{1}{2}\arcsin(a_1) - \frac{1}{4}\sin(2\arcsin(a_1))\right) & \text{if} \quad -1 < a_1 < 1 \\[2ex]
0 & \text{if} \quad a_1 \geq 1
\end{cases}
\end{aligned}
$$

and

$$
\begin{aligned}
I_2 &= \int_{\xi<0} \xi \sqrt{h^n_{i+1}}\, \chi\Big(\frac{\xi - u^n_{i+1}}{\sqrt{h^n_{i+1}}}\Big)\, d\xi \\
&= \sqrt{h^n_{i+1}}\, \frac{\sqrt{2}}{\pi\sqrt{\beta}} \int_{\xi<0} \xi \left(1 - \left(\frac{\xi - u^n_{i+1}}{\sqrt{2\beta h^n_{i+1}}}\right)^2\right)^{1/2}_{+} d\xi \\
&= \begin{cases}
0 & \text{if} \quad a_2 \leq -1 \\[2ex]
-\frac{2}{3\pi}\sqrt{2\beta}\,(h^n_{i+1})^{3/2}\ \cos^3(\arcsin(a_2)) & \\
+\frac{2}{\pi}\,(hu)^n_{i+1} \left(\frac{\pi}{4} + \frac{1}{2}\arcsin(a_2) + \frac{1}{4}\sin(2\arcsin(a_2))\right) & \text{if} \quad -1 < a_2 < 1 \\[2ex]
(hu)^n_{i+1} & \text{if} \quad a_2 \geq 1
\end{cases}
\end{aligned}
$$

using $a_1 := -u^n_i/\sqrt{2\beta h^n_i}$ and $a_2 := -u^n_{i+1}/\sqrt{2\beta h^n_{i+1}}$.
For the second component we get

$$
\begin{aligned}
(F^n_{i+1/2})^2 &= \int_{\xi\geq 0} \xi^2\, M^n_i(\xi)\, d\xi + \int_{\xi<0} \xi^2\, M^n_{i+1}(\xi)\, d\xi \\
&= \underbrace{\int_{\xi\geq 0} \xi^2\, M(h^n_i, \xi - u^n_i)\, d\xi}_{I_3} + \underbrace{\int_{\xi<0} \xi^2\, M(h^n_{i+1}, \xi - u^n_{i+1})\, d\xi}_{I_4}\ .
\end{aligned}
$$

And the integrals I_3 and I_4 are

$$I_3 = \begin{cases} h_i^n (u_i^n)^2 + \frac{1}{2}\beta (h_i^n)^2 & \text{if} \quad a_1 \leq -1 \\ \frac{4}{\pi}\,\beta\,(h_i^n)^2 \Big(\frac{\pi}{16} - \frac{1}{8}\arcsin(a_1) + \frac{1}{32}\sin(a_1) \Big) & \\ -\frac{4}{3\pi}\sqrt{2\beta}\,(hu)_i^n \sqrt{h_i^n}\,\cos^3(\arcsin(a_1)) & \\ +\frac{2}{\pi}\,h_i^n (u_i^n)^2 \left(\frac{\pi}{4} - \frac{1}{2}\arcsin(a_1) - \frac{1}{4}\sin(2\arcsin(a_1)) \right) & \text{if} \quad -1 < a_1 < 1 \\ 0 & \text{if} \quad a_1 \geq 1 \end{cases}$$

$$I_4 = \begin{cases} 0 & \text{if} \quad a_2 \leq -1 \\ \frac{4}{\pi}\,\beta\,(h_{i+1}^n)^2 \left(\frac{1}{8}\arcsin(a_2) + \frac{\pi}{16} - \frac{1}{32}\sin(4\arcsin(a_2)) \right) & \\ -\frac{4}{3\pi}\sqrt{2\beta}\,(hu)_{i+1}^n \sqrt{h_{i+1}^n}\,\cos^3(\arcsin(a_2)) & \\ +\frac{2}{\pi}\,h_{i+1}^n (u_{i+1}^n)^2 \left(\frac{\pi}{4} + \frac{1}{2}\arcsin(a_2) + \frac{1}{4}\sin(2\arcsin(a_2)) \right) & \text{if} \quad -1 < a_2 < 1 \\ h_{i+1}^n (u_i^n)^2 + \frac{1}{2}\beta\,(h_{i+1}^n)^2 & \text{if} \quad a_2 \geq 1 \end{cases}$$

With these informations our first scheme reads:

Scheme 1

$$U_i^{n+1} = U_i^n - \lambda\big(F_{i+1/2}^n - F_{i-1/2}^n\big) + \Delta t\, S_i^n$$

where

$$F_{i+1/2}^n = \big((F_{i+1/2}^n)^1, (F_{i+1/2}^n)^2\big)^T = \big(I_1 + I_2, I_3 + I_4\big)^T \ ,$$

$$S_i^n = \begin{cases} \begin{pmatrix} 0 \\ \tilde{g}_i^n\, h_i^{n+1} \end{pmatrix} & \textit{if} \quad u_i^n = 0 \\ \\ \begin{pmatrix} 0 \\ g(u_i^n)\, h_i^{n+1} \end{pmatrix} & \textit{if} \quad u_i^n \neq 0 \ , \end{cases}$$

$$\tilde{g}_i^n = \min\Big[\sin\zeta + R,\ \max\Big(\beta\big((h_{i+1}^n - h_{i-1}^n)/2\Delta x\big), \sin\zeta - R\Big)\Big]$$

and

$$R = \cos\zeta\ \tan\delta\ .$$

Obviously the scheme is conservative in the first component and consistent since we can write for the numerical flux function

$$F^n_{i+1/2} = F(U^n_i, U^n_{i+1})$$

where

$$F(U,V) = \int_{\xi \geq 0} \begin{pmatrix} 1 \\ \xi \end{pmatrix} \xi \, M\big(U_1, \xi - \frac{U_2}{U_1}\big) \, d\xi + \int_{\xi < 0} \begin{pmatrix} 1 \\ \xi \end{pmatrix} \xi \, M\big(V_1, \xi - \frac{V_2}{V_1}\big) \, d\xi \ ,$$

with $U, V \in \mathbb{R}^2$ and the indices denote the first and second component, respectively. Therefore we get for $U = (h, hu)^T$

$$\begin{aligned} F(U,U) &= \int_{\mathbb{R}} \begin{pmatrix} 1 \\ \xi \end{pmatrix} \xi \, M(h, \xi - u) \, d\xi \\ &= \begin{pmatrix} hu \\ hu^2 + \frac{1}{2}\beta h^2 \end{pmatrix} \ . \end{aligned}$$

If we now consider an admissible profile h at time t_n and insert $u^n_i = 0$ into the method, we get

$$\begin{aligned} h^{n+1}_i &= h^n_i - \lambda \left[(F^n_{i+1/2})^1 - (F^n_{i-1/2})^1 \right] \\ &= h^n_i - \lambda \left[\frac{2}{3\pi}\sqrt{2\beta} \left((h^n_i)^{3/2} - (h^n_{i+1})^{3/2} \right) - \frac{2}{3\pi}\sqrt{2\beta} \left((h^n_{i-1})^{3/2} - (h^n_i)^{3/2} \right) \right] \\ &= h^n_i + \lambda \left[\frac{2}{3\pi}\sqrt{2\beta} \left((h^n_{i+1})^{3/2} - 2(h^n_i)^{3/2} + (h^n_{i-1})^{3/2} \right) \right] \ . \end{aligned}$$

Since the second term on the right hand side does not vanish in general, we get $h^{n+1}_i \neq h^n_i$. So this simple scheme does not preserve the desired steady states. Note that the verification whether a profile is admissible takes place in the discretized source term, which influences only the second component. We are looking for a method, that ensures

$$u^n_i = 0 \ \ \forall i \in \mathbb{Z} \quad \Longrightarrow \quad h^{n+1}_i = h^n_i \ \ \forall i \in \mathbb{Z} \ ,$$

i.e. that changes inadmissible profiles via the velocity. In addition we want

$$u^n_i = 0 \quad \forall i \in \mathbb{Z} \quad \Longrightarrow \quad u^{n+1}_i = 0 \quad \forall i \in \mathbb{Z} \ .$$

for admissible profiles.
This can be reached by little modifications in the microscopic flux function and the discretization of the source term. As new microscopic fluxes we choose

$$\tilde{M}^n_{i+1/2} = \begin{cases} M\left(\frac{h_i^n+h_{i+1}^n}{2}, \xi - u_i^n\right) & \text{für } \xi \geq 0 \\ M\left(\frac{h_i^n+h_{i+1}^n}{2}, \xi - u_{i+1}^n\right) & \text{für } \xi < 0 \end{cases}$$

$$= \begin{cases} \sqrt{\frac{h_i^n+h_{i+1}^n}{2}}\,\chi\left(\frac{\xi-u_i^n}{\sqrt{(h_i^n+h_{i+1}^n)/2}}\right) & \text{für } \xi \geq 0 \\ \sqrt{\frac{h_i^n+h_{i+1}^n}{2}}\,\chi\left(\frac{\xi-u_{i+1}^n}{\sqrt{(h_i^n+h_{i+1}^n)/2}}\right) & \text{für } \xi < 0\ . \end{cases} \tag{25}$$

That means that the actual upwinding takes place only in the velocity u and no longer in the height h. With (25) the new macroscopic fluxes $\tilde{F}^n_{i+1/2} = \left((\tilde{F}^n_{i+1/2})^1, (\tilde{F}^n_{i+1/2})^2\right)^T$ read

$$\begin{aligned} (\tilde{F}^n_{i+1/2})^1 &= \int_{\mathbb{R}} \xi\, M^n_{i+1/2}(\xi)\, d\xi \\ &= \underbrace{\int_{\xi\geq 0} \xi \sqrt{\frac{h_i^n + h_{i+1}^n}{2}}\,\chi\left(\frac{\xi - u_i^n}{\sqrt{(h_i^n + h_{i+1}^n)/2}}\right) d\xi}_{\tilde{I}_1} \\ &+ \underbrace{\int_{\xi<0} \xi \sqrt{\frac{h_i^n + h_{i+1}^n}{2}}\,\chi\left(\frac{\xi - u_{i+1}^n}{\sqrt{(h_i^n + h_{i+1}^n)/2}}\right) d\xi}_{\tilde{I}_2} \end{aligned}$$

and

$$\begin{aligned} (\tilde{F}^n_{i+1/2})^2 &= \int_{\mathbb{R}} \xi^2\, M^n_{i+1/2}(\xi)\, d\xi \\ &= \underbrace{\int_{\xi\geq 0} \xi^2 \sqrt{\frac{h_i^n + h_{i+1}^n}{2}}\,\chi\left(\frac{\xi - u_i^n}{\sqrt{(h_i^n + h_{i+1}^n)/2}}\right) d\xi}_{\tilde{I}_3} \\ &+ \underbrace{\int_{\xi<0} \xi^2 \sqrt{\frac{h_i^n + h_{i+1}^n}{2}}\,\chi\left(\frac{\xi - u_{i+1}^n}{\sqrt{(h_i^n + h_{i+1}^n)/2}}\right) d\xi}_{\tilde{I}_4}\ . \end{aligned}$$

By defining $\tilde{a}_1 := -u_i^n/\sqrt{\beta(h_i^n + h_{i+1}^n)}$ and $\tilde{a}_2 := -u_{i+1}^n/\sqrt{\beta(h_i^n + h_{i+1}^n)}$ and after some easy computations we get

$$
\tilde{I}_1 = \begin{cases} \left(\frac{h_i^n+h_{i+1}^n}{2}\right) u_i^n & \text{if} \quad \tilde{a}_1 \le -1 \\ \frac{2}{3\pi}\sqrt{2\beta}\left(\frac{h_i^n+h_{i+1}^n}{2}\right)^{3/2} \cos^3(\arcsin(\tilde{a}_1)) & \\ +\frac{2}{\pi}\left(\frac{h_i^n+h_{i+1}^n}{2}\right) u_i^n \left(\frac{\pi}{4} - \frac{1}{2}\arcsin(\tilde{a}_1)\right. & \\ \left. -\frac{1}{4}\sin(2\arcsin(\tilde{a}_1))\right) & \text{if} \quad -1 < \tilde{a}_1 < 1 \\ 0 & \text{if} \quad \tilde{a}_1 \ge 1 \ , \end{cases}
$$

$$
\tilde{I}_2 = \begin{cases} 0 & \text{if} \quad \tilde{a}_2 \le -1 \\ -\frac{2}{3\pi}\sqrt{2\beta}\left(\frac{h_i^n+h_{i+1}^n}{2}\right)^{3/2} \cos^3(\arcsin(\tilde{a}_2)) & \\ +\frac{2}{\pi}\left(\frac{h_i^n+h_{i+1}^n}{2}\right) u_{i+1}^n \left(\frac{\pi}{4} + \frac{1}{2}\arcsin(\tilde{a}_2)\right. & \\ \left. +\frac{1}{4}\sin(2\arcsin(\tilde{a}_2))\right) & \text{if} \quad -1 < \tilde{a}_2 < 1 \\ \left(\frac{h_i^n+h_{i+1}^n}{2}\right) u_{i+1}^n & \text{if} \quad \tilde{a}_2 \ge 1 \ , \end{cases}
$$

$$
\tilde{I}_3 = \begin{cases} \left(\frac{h_i^n+h_{i+1}^n}{2}\right)(u_i^n)^2 + \frac{1}{2}\beta\left(\frac{h_i^n+h_{i+1}^n}{2}\right)^2 & \text{if} \quad \tilde{a}_1 \le -1 \\ \frac{4}{\pi}\beta\left(\frac{h_i^n+h_{i+1}^n}{2}\right)^2 \left(\frac{\pi}{16} - \frac{1}{8}\arcsin(\tilde{a}_1) + \frac{1}{32}\sin(4\arcsin(\tilde{a}_1))\right) & \\ +\frac{4}{3\pi}\sqrt{2\beta}\left(\frac{h_i^n+h_{i+1}^n}{2}\right)^{3/2} u_i^n \cos^3(\arcsin(\tilde{a}_1)) & \\ +\frac{2}{\pi}\left(\frac{h_i^n+h_{i+1}^n}{2}\right)(u_i^n)^2 \left(\frac{\pi}{4} - \frac{1}{2}\arcsin(\tilde{a}_1) - \frac{1}{4}\sin(2\arcsin(\tilde{a}_1))\right) & \text{if} \quad -1 < \tilde{a}_1 < 1 \\ 0 & \text{if} \quad \tilde{a}_1 \ge 1 \end{cases}
$$

and

$$
\tilde{I}_4 = \begin{cases} 0 & \text{if} \quad \tilde{a}_2 \le -1 \\ \frac{4}{\pi}\beta\left(\frac{h_i^n+h_{i+1}^n}{2}\right)^2 \left(\frac{\pi}{16} + \frac{1}{8}\arcsin(\tilde{a}_2) - \frac{1}{32}\sin(4\arcsin(\tilde{a}_2))\right) & \\ -\frac{4}{3\pi}\sqrt{2\beta}\left(\frac{h_i^n+h_{i+1}^n}{2}\right)^{3/2} u_{i+1}^n \cos^3(\arcsin(\tilde{a}_2)) & \\ +\frac{2}{\pi}\left(\frac{h_i^n+h_{i+1}^n}{2}\right)(u_{i+1}^n)^2 \left(\frac{\pi}{4} + \frac{1}{2}\arcsin(\tilde{a}_2) + \frac{1}{4}\sin(2\arcsin(\tilde{a}_2))\right) & \text{if} \quad -1 < \tilde{a}_2 < 1 \\ \left(\frac{h_i^n+h_{i+1}^n}{2}\right)(u_{i+1}^n)^2 + \frac{1}{2}\beta\left(\frac{h_i^n+h_{i+1}^n}{2}\right)^2 & \text{if} \quad \tilde{a}_2 \ge \ . \end{cases}
$$

If we now assume $u_i^n = 0 \ \forall i \in \mathbb{Z}$ we get for the first component of the modified flux

$$
\begin{aligned}
(\tilde{F}^n_{i+1/2})^1 &= \tilde{I}_1 + \tilde{I}_2 \\
&= \frac{2}{3\pi}\sqrt{2\beta}\left(\frac{h^n_i + h^n_{i+1}}{2}\right)^{3/2} - \frac{2}{3\pi}\sqrt{2\beta}\left(\frac{h^n_i + h^n_{i+1}}{2}\right)^{3/2} \\
&= 0 \qquad\qquad \forall i \in \mathbb{Z}
\end{aligned}
$$

and therefore

$$
\begin{aligned}
h^{n+1}_i &= h^n_i - \lambda\left[(\tilde{F}^n_{i+1/2})^1 - (\tilde{F}^n_{i-1/2})^1\right] \\
&= h^n_i \qquad\qquad \forall i \in \mathbb{Z}\ .
\end{aligned}
$$

As desired the height profile does not change for vanishing velocities. Now we want to change the discretization of the source term for $u^n_i = 0$ such that we get $u^{n+1}_i = 0$ for admissible profiles. In that case the second component of the modified flux reads

$$
\begin{aligned}
(\tilde{F}^n_{i+1/2})^2 &= \frac{4}{\pi}\beta\left(\frac{h^n_i + h^n_{i+1}}{2}\right)^2\left(\frac{\pi}{16}\right) + \frac{4}{\pi}\beta\left(\frac{h^n_i + h^n_{i+1}}{2}\right)^2\left(\frac{\pi}{16}\right) \\
&= \frac{\beta}{2}\left(\frac{h^n_i + h^n_{i+1}}{2}\right)^2 .
\end{aligned}
$$

Inserting that into the method the moment becomes to

$$
\begin{aligned}
(hu)^{n+1}_i &= (hu)^n_i - \lambda\left[(\tilde{F}^n_{i+1/2})^2 - (\tilde{F}^n_{i-1/2})^2\right] + \Delta t\, \tilde{g}^n_i\, h^{n+1}_i \\
&= -\lambda\frac{\beta}{2}\left[\left(\frac{h^n_i + h^n_{i+1}}{2}\right)^2 - \left(\frac{h^n_{i-1} + h^n_i}{2}\right)^2\right] + \Delta t\, \tilde{g}^n_i\, h^{n+1}_i \\
&= -\Delta t\, \beta\left(\frac{h^n_{i+1} - h^n_{i-1}}{2\Delta x}\right)\left(\frac{h^n_{i+1} + 2h^n_i + h^n_{i-1}}{4}\right) + \Delta t\, \beta\left(\frac{h^n_{i+1} - h^n_{i-1}}{2\Delta x}\right) h^{n+1}_i\ .
\end{aligned} \tag{26}
$$

So if we approximate

$$
h^{n+1}_i \approx \left(\frac{h^n_{i+1} + 2h^n_i + h^n_{i-1}}{4}\right), \tag{27}
$$

we get for admissible profiles $u^{n+1}_i = u^n_i\ \forall i \in \mathbb{Z}$. Note that if we have an inadmissible mass at rest the height remains unchanged in the following step, but will change in the next step due to the velocity, so that the approximation made above for h^{n+1}_i makes sense.

Now we want to check whether the method is able to pass into the state of an equilibrium for descending height gradients and small velocities. For small velocities u the moments equation reads

$$
q^{n+1}_i = q^n_i - \lambda\left[(\tilde{F}^n_{i+1/2})^2 - (\tilde{F}^n_{i-1/2})^2\right] + \Delta t\, g(u^n_i)\, h^{n+1}_i\ .
$$

Usually the first expressions on the right hand side will be small, but the last one can be significantly large to avoid the decay of the moment. Since we have $g^n_i = g(u^n_i)$ for $u^n_i \neq 0$, where

$$g(u) = \sin\zeta - \mathrm{sgn}(u)\, R = \sin\zeta - \mathrm{sgn}(u)\, \cos\zeta\, \tan\delta\ ,$$

g_i^n always has opposite sign to u_i^n for $\tan\zeta < \tan\delta$. For small moments q_i^n the contribution of g_i^n will cause a change of sign at least after some time steps. That means that friction would be able to change the sign of the velocity, what does not make sense from a physical point of view. Of course we could set $q_i^{n+1} = 0$ for sufficiently small q_i^n, but then our method would not be able to start sliding. So to enable the scheme to stop a sliding granular mass we take the approximation (27) not only for $u = 0$ but for all $|q_i^n| = |(hu)_i^n| < |\Delta t\, g(u_i^n)\, h_i^{n+1}|$.
Moreover we can extent the scheme in using a convex combination in the case of $|q_i^n| < |\Delta t\, g(q_i^n)\, h_i^{n+1}|$ of the two discretizations of the source term

$$\Delta t\, \tilde{g}_i^n \left((h_{i+1}^n + 2h_i^n + h_{i-1}^n)/4\right)$$

and

$$\Delta t\, g(q_i^n)\, h_i^{n+1}$$

with the coefficients

$$(1-\mu) = \left(1 + q_i^n/\Delta t\, g(q_i^n)\, h_i^{n+1}\right)$$

and

$$\mu = -q_i^n/\Delta t\, g(q_i^n)\, h_i^{n+1}\ ,$$

respectively. The smaller the velocity the more we use the discretized source term for $u_i^n = 0$ whereas the influence of the source term for moving masses decreases. For simplification we write the resulting method in its two components.

Scheme 2

$$h_i^{n+1} = h_i^n - \lambda\left((\tilde{F}_{i+1/2}^n)^1 - (\tilde{F}_{i-1/2}^n)^1\right)\ ,$$

$$q_i^{n+1} = \begin{cases} -\lambda\left((\tilde{F}_{i+1/2}^n)^2 - (\tilde{F}_{i-1/2}^n)^2\right) & \\ +(1-\mu)\,\Delta t\, \tilde{g}_i^n\left((h_{i+1}^n + 2h_i^n + h_{i-1}^n)/4\right) & \textit{if} \quad |q_i^n| < |\Delta t\, g(q_i^n)\, h_i^{n+1}| \\ & \\ q_i^n - \lambda\big((\tilde{F}_{i+1/2}^n)^2 - (\tilde{F}_{i-1/2}^n)^2\big) + \Delta t\, g(q_i^n)\, h_i^{n+1} & \textit{if} \quad |q_i^n| \geq |\Delta t\, g(q_i^n)\, h_i^{n+1}| \end{cases}$$

where

$$\tilde{g}_i^n = \min\left[\sin\zeta + R,\ \max\Big(\beta\big((h_{i+1}^n - h_{i-1}^n)/2\Delta x\big), \sin\zeta - R\Big)\right]\ .$$

The numerical fluxes are given by

$$\tilde{F}_{i+1/2}^n = \left((\tilde{F}_{i+1/2}^n)^1, (\tilde{F}_{i+1/2}^n)^2\right)^T = \left(\tilde{I}_1 + \tilde{I}_2, \tilde{I}_3 + \tilde{I}_4\right)^T$$

and $\tilde{I}_1$–$\tilde{I}_4$ computed above.

3.3 The coupled method

Unfortunately the last method causes oscillations in the case of strongly inadmissible initial profiles as Riemann problems. These oscillations are quite small and seem to be stable, but do not decay in time. Perhaps the use of mean values for h in the microscopic numerical fluxes is responsible for that oscillations. To get rid of this drawback we modify our last scheme once more. In the next section we compare the numerical results for the classical Riemann problem with the exact solution. The oscillations caused by scheme 2 are distinguished clearly.
But the modification of our first method was reasoned only by the request to preserve the steady states and to simulate the starting and stopping of a granular mass. Masses at high rates are obviously far away from stopping or passing into an equilibrium. Therefore the use of the modificated scheme is not necessary in that case. This leads us to a combination of the both schemes, the first one for masses in rapid flows and the modificated scheme for the simulation of starting or stopping masses or those in an equilibrium. The coupled method reads

Scheme 3

$$\left.\begin{aligned} h_i^{n+1} &= h_i^n - \lambda\big((\tilde{F}_{i+1/2}^n)^1 - (\tilde{F}_{i-1/2}^n)^1\big) \\ q_i^{n+1} &= -\lambda\big((\tilde{F}_{i+1/2}^n)^2 - (\tilde{F}_{i-1/2}^n)^2\big) \\ &\quad +(1-\mu)\,\Delta t\,\tilde{g}_i^n\,\big((h_{i+1}^n + 2h_i^n + h_{i-1}^n)/4\big) \end{aligned}\right\} \quad \textit{if} \;\; |q_i^n| < |\Delta t\, g(q_i^n)\, h_i^{n+1}|\;,$$

$$\left.\begin{aligned} h_i^{n+1} &= h_i^n - \lambda\big((F_{i+1/2}^n)^1 - (F_{i-1/2}^n)^1\big) \\ q_i^{n+1} &= q_i^n - \lambda\big((F_{i+1/2}^n)^2 - (F_{i-1/2}^n)^2\big) + \Delta t\, g(q_i^n)\, h_i^{n+1} \end{aligned}\right\} \quad \textit{if} \;\; |q_i^n| \geq |\Delta t\, g(q_i^n)\, h_i^{n+1}|$$

where

$$\tilde{g}_i^n = \min\Big[\sin\zeta + R,\, \max\Big(\beta\big((h_{i+1}^n - h_{i-1}^n)/2\Delta x\big), \sin\zeta - R\Big)\Big]\;,$$

$$\tilde{F}_{i+1/2}^n = \big((\tilde{F}_{i+1/2}^n)^1, (\tilde{F}_{i+1/2}^n)^2\big)^T = \big(\tilde{I}_1 + \tilde{I}_2, \tilde{I}_3 + \tilde{I}_4\big)^T$$

and

$$F_{i+1/2}^n = \big((F_{i+1/2}^n)^1, (F_{i+1/2}^n)^2\big)^T = \big(I_1 + I_2, I_3 + I_4\big)^T\;.$$

In [8] the authors formulate a theorem for their kinetic method solving the shallow water equations with a source, that ensures nonnegativity of the height h. Because our first method was constructed following the Ansatz made in [8], we can easily apply that theorem to the coupled method in the case of rapid flows.

Theorem 3 *Under the CFL condition*

$$\max_{i\in\mathbb{Z}} \left(|u_i^n| + \sqrt{2\beta h_i^n}\right) \leq \frac{\Delta x}{\Delta t} = \frac{1}{\lambda} \quad \textit{and} \quad |q_i^n| \geq |\Delta t\, g(q_i^n)\, h_i^{n+1}| \tag{28}$$

the coupled scheme 3 keeps the height h of the granular mass nonnegative, that means we have $h_i^n \geq 0\ \forall i \in \mathbb{Z}\ \forall n \in \mathbb{N}$, if $h_i^0 \geq 0\ \forall i \in \mathbb{Z}$.

Otherwise the considered mass is only moving very slowly or not at all, so we can expect that the height is kept nonnegative, too. Several numerical tests of the method can be found in the next section.

4 Numerical tests

In this section we want to test the scheme numerically. Thereby the emphasis lies on the preservation of the steady states of granular masses at rest as well as the starting of inadmissible profiles and the stopping of the masses after deformation. Throughout the tests we choose $\varepsilon = 0.4$, $\Delta x = 0.05$ and $\Delta t = 0.001$ as long as we do not give other values.

- We start with the classical Riemann problem for the SH equations without a source, i.e. $\zeta = \delta = 0$, and the initial data

  $$\begin{aligned} h(0,x) &= \begin{cases} h_l & \text{if } x \leq x_0 \\ h_r & \text{if } x > x_0 \end{cases} \\ u(0,x) &= 0, \end{aligned}$$

  where $h_l = 1$ and $h_r = 0.5$. The exact solution for this problem is given by

  $$h(x,t) = \begin{cases} h_l & \text{if } \ x \leq \lambda_l^1\, t + x_0 \\ \frac{1}{9\beta}\left[\left(u_l + 2\sqrt{\beta h_l}\right) - \left(\frac{x-x_0}{t}\right)\right]^2 & \text{if } \ \lambda_l^1\, t + x_0 < x \leq \lambda_m^1\, t + x_0 \\ h_m & \text{if } \ \lambda_m^1\, t + x_0 < x \leq s\, t + x_0 \\ h_r & \text{if } \ x > s\, t + x_0\ , \end{cases}$$

  $$u(x,t) = \begin{cases} u_l & \text{if } \ x \leq \lambda_l^1\, t + x_0 \\ \frac{2}{3}\left[\left(\frac{x-x_0}{t}\right) + \sqrt{\beta h_l} - \frac{1}{2}u_l\right] & \text{if } \ \lambda_l^1\, t + x_0 < x \leq \lambda_m^1\, t + x_0 \\ u_m & \text{if } \ \lambda_m^1\, t + x_0 < x \leq s\, t + x_0 \\ u_r & \text{if } \ x > s\, t + x_0 \end{cases}$$

  and λ_l^1, λ_m^1 and λ_r^1 are defined as

  $$\lambda_l^1 = \lambda^1(h_l, u_l)\ , \quad \lambda_m^1 = \lambda^1(h_m, u_m)\ , \quad \lambda_r^1 = \lambda^1(h_r, u_r)\ ,$$

  where $\lambda^1(h,u) = u - \sqrt{\beta h}$ denotes the first eigenvalue of the SH equations (1) in quasilinear form and $s = \frac{h_m u_m - h_r u_r}{h_m - h_r}$ denotes the shock speed. For 5000 time steps the results computed with scheme 3 are compared with the exact solution in Fig. 1.

- The next test problem can be seen as a one dimensional breaking grain silo. The initial data for this Riemann problem are given as

$$\begin{aligned} h(0,x) &= \begin{cases} h_l & \text{if } x \leq x_1 \\ h_m & \text{if } x_1 < x \leq x_2 \\ h_r & \text{if } x > x_2 \end{cases} \\ u(0,x) &= 0, \end{aligned}$$

where $h_l = h_r = 0.3$ and $h_m = 2.3$. Moreover we choose $\zeta = 0$, $\delta = \pi/10$ and consider 10000 time steps. We expect the mass to move symmetrically until the gradients of the height profile are sufficiently small to be recognized by the method as gradients of an equilibrium. That means the grain begins to move, but has to stop after a while because of the friction. The results can be seen for different times in figure 2, the time evolution is given in Fig. 3.

- Next we consider the previous Riemann problem over an incline with inclination and friction angle of $\zeta = \pi/15$ and $\delta = \pi/5$. Now we expect the mass no longer to move symmetrically, but more to the right. For 8000 time steps the results are shown in figure 4 in a three dimensional view.

- As a fourth example we consider the parabolic initial data

$$\begin{aligned} h(0,x) &= \max\left(K/10,\ K - l\,(x-x_0)^2\right) \\ u(0,x) &= 0 \end{aligned}$$

where

$$K = 1\ , \quad l = 4\ ,$$

There is no inclination, that means $\zeta = 0$, and as a friction angle we fix $\delta = \pi/15$. The results for 6000 time steps can be seen in figure 5 in a threedimensional view. Like the profile in the second example the mass is moving symmetrically and stops after a while.

- Finally we want to compare the results for the initial data

$$\begin{aligned} h_0(x) &= \begin{cases} \max\left(0.9\,\sin[\pi(x-0.6)] - 0.3\,\sin[2\,\pi(x-0.6)], 0.1\right) & \text{if } \ 0.6 < x < 1.6 \\ 0.1 & \text{otherwise} \end{cases} \\ u(0,x) &= 0 \end{aligned}$$

where $\varepsilon = 0.3218$, $\zeta = \pi/6 = 30°$ and $\delta = \pi/18 = 10°$ with the results in [10] for nearly the same problem. Because of $\zeta > \delta$ the mass starts moving, but, in contrary to the previous examples, does not stop and accelerates roughly constantly. The results for

4000 time steps are shown in figure 6 and are very similar to the computations in [10], where the authors apply a finite difference scheme of MacCormack. The fragmentation of the initial profile into two smaller and spreading profiles seems to be typical for such problems and occurs for the presented method applied to other initial data of the above type, too. Nevertheless the authors in [10] are doubtful concerning the accuracy of the results.

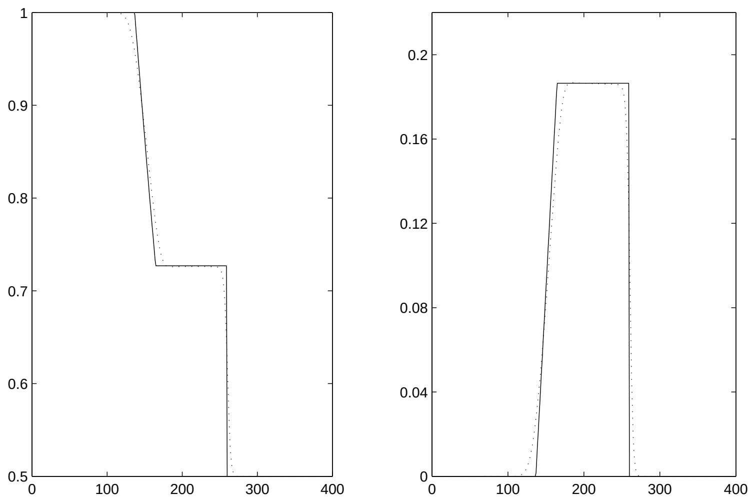

Figure 1: Comparison of exact (solid line) and numerical solution (dotted line) computed by scheme 3 for Riemann problem with $\zeta = \delta = 0$.

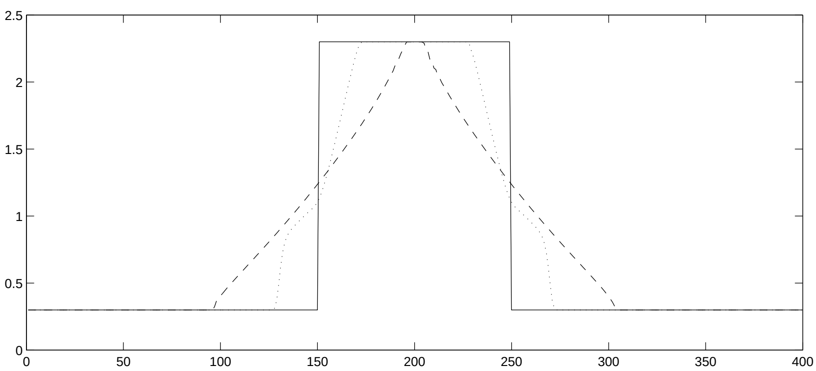

Figure 2: Initial height profile (solid line), height profile after 1100 time steps (dotted line) and final height profile (dashed line).

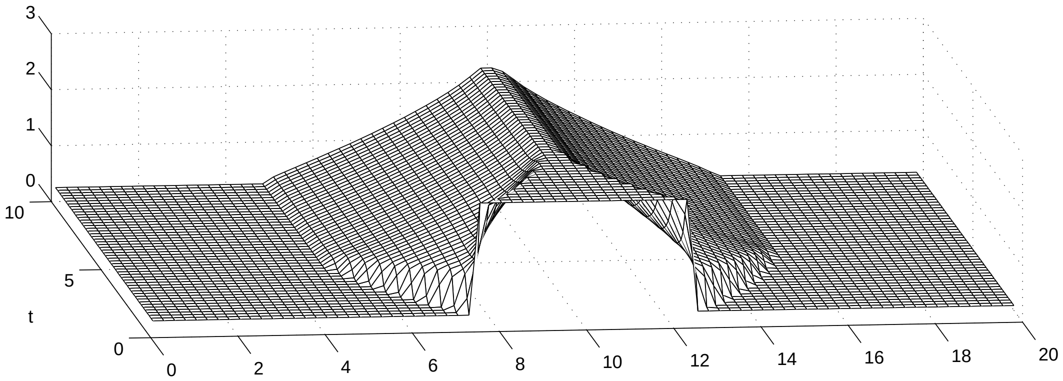

Figure 3: Time evolution of the height h.

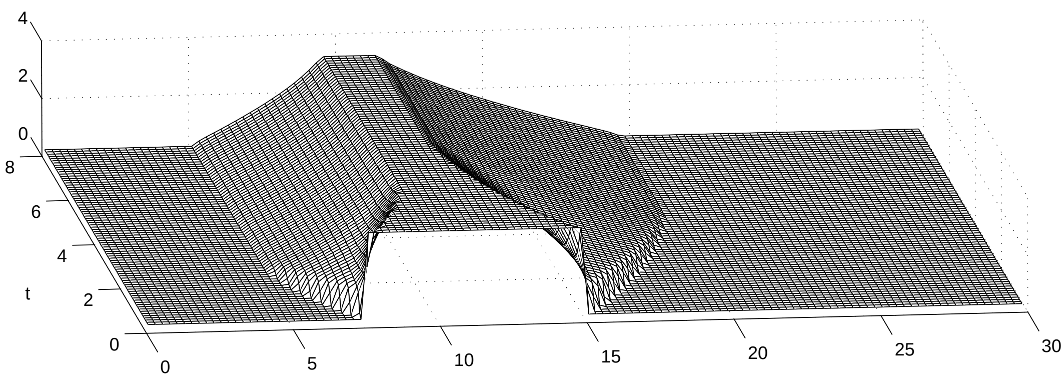

Figure 4: Time evolution of the height h for the Riemann problem over an incline.

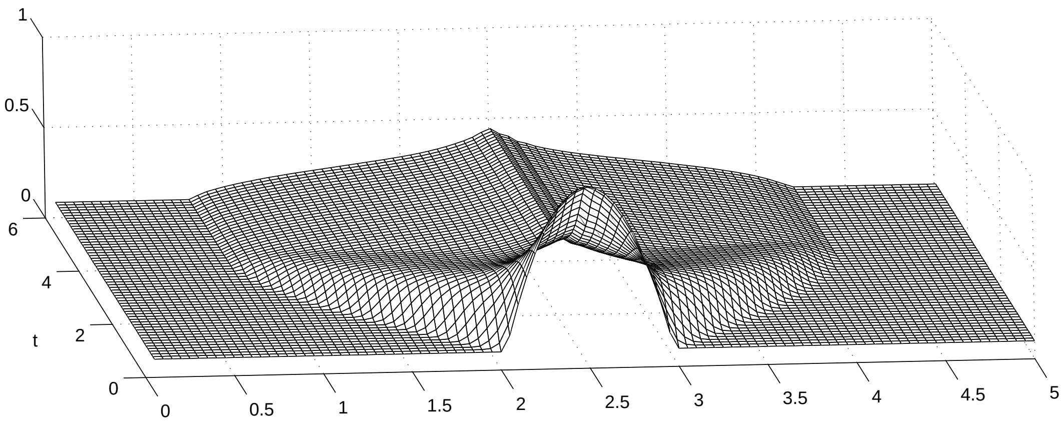

Figure 5: Time evolution of the height h for a parabolic initial profile.

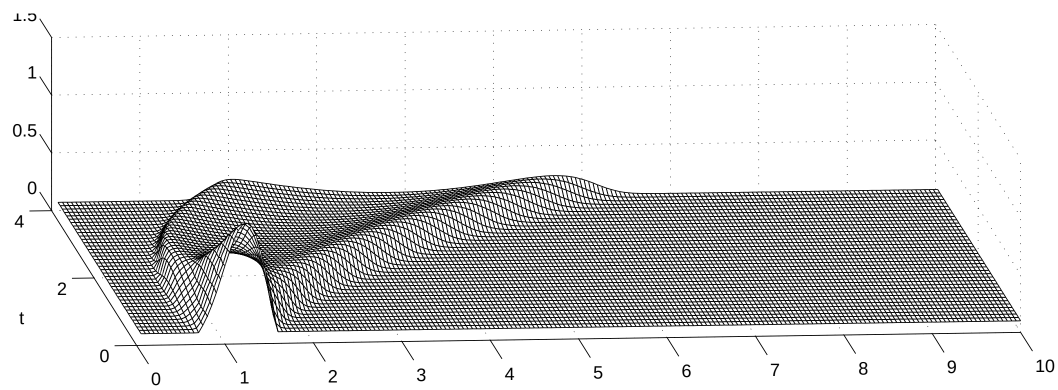

Figure 6: Spreading and constant acceleration of the height h for a sinosoidal initial profile.

5 Conclusion

In this paper we presented a numerical method for the SH equations for constant inclination angles based on the kinetic formulation of these equations. Moreover we were able to give a kinetic formulation for the general SH equations describing the motion of granular material over smoothly varying chutes. For the construction of the scheme we followed an Ansatz of Perthame and Simeoni ([8]). The resulting method is able to preserve the steady states of granular masses at rest and to describe the beginning and stopping of the motion of other solutions. Moreover we could adopt a theorem of Perthame and Simeoni ([8]), which ensures the nonnegativity of the height of the granular material at least in regions of large deformations. The method was testet on several examples.

Improvements and generalizations of the method are possible: a generalization to the two dimensional case, for example, as well as the construction of a higher order method and, with regard to the last example, the integration of a suitable entropy criteria. Furthermore, one could use other, more sophisticated friction models than the Coulomb friction model as done in [5] for the shallow water equations.

References

[1] Balean,R.: Granular avalanche flow down a smoothly varying slope: the existence of entropy solutions

[2] Cercignani,C., Illner,R., Pulvirenti,M.: The Mathematical Theory of Dilute Gases. Springer (1994)

[3] Katsaounis,Th., Perthame,B., Simeoni,C.: Upwinding Sources at Interfaces in conservation laws. Appl.Math.Lett. (2003)

[4] Mangeney-Castelnau,A., Vilotte,J.P., Bristeau,M.O., Bouchut,F., Perthame,B., Simeoni,C., Yernini,S.: A new kinetic scheme for Saint-Venant equations applied to debris avalanches. INRIA: Rapport de recherche n° 4646 (2002)

[5] Mangeney-Castelnau,A., Vilotte,J.P., Bristeau,M.O., Bouchut,F., Perthame,B., Simeoni,C., Yernini,S.: Numerical modeling of avalanches based on Saint-Venant equations using a kinetic scheme. Journal of Geophysical Research, Vol. 108, No.B11, 2527 (2003)

[6] Mangeney-Castelnau,A., Bouchut,F., Vilotte,J.P., Aubertin,A., Pirulli,M.: On the use of Saint Venant equations to simulate the spreading of a granular mass. Journal of Geophysical Research, Vol. 110, B09103 (2005)

[7] Perthame,B.: Kinetic Formulation of Conservation Laws. Oxford University Press (2002)

[8] Perthame,B., Simeoni,C.: A kinetic scheme for the Saint-Venant system with a source term. Calcolo 38, 201-231 (2001)

[9] Perthame,B., Simeoni,C.: Convergence of the Upwind Interface Source method for hyperbolic conservation laws. Springer (2003)

[10] Savage,S.B., Hutter,K.: The motion of a finite mass of granular material down a rough incline. J. Fuid Mech. (1998), vol. 199, pp. 177-215

[11] Savage,S.B., Hutter,K.: The dynamics of avalanches of granular materials from initiation to runout. Part 1: Analysis. Acta Mechanica (1991), vol. 86, pp. 201-223

[12] Struckmeier,J.: On a kinetic Model for Shallow Water Waves. Mathematical Methods in the Appl. Sciences, Vol.18 (1995) 709-722